23rd ABCM International Congress of Mechanical Engineering
December 6-11, 2015, Rio de Janeiro, RJ, Brazil

UNCERTAINTY ANALYSIS DURING VAPOR FLOW INSIDE MPE MICROCHANNELS

Jeferson Diehl de Oliveira
jdiehl@lepten.ufsc.br
Guilherme Piazza Zanette
zanette.gui.eng@hotmail.com
Polyana Werncke Coan
polyanacoan@gmail.com
Júlio César Passos
julio.passos@ufsc.br
Saulo Güths
saulo@lmpt.ufsc.br
Federal University of Santa Catarina – Florianópolis - SC - Brazil

Jacqueline Biancon Copetti
jcopetti@unisinos.br
Mechanical Engineering Graduate Program - University of Vale do Rio dos Sinos – São Leopoldo - RS – Brazil

Abstract. *This paper reports a study about uncertainties related to vapor flow in micro-channels using fluid refrigerant R134a. Heat exchangers involving these micro-channels are more efficient than conventional ones, in addition to having reduced the refrigerant inventory. The main goal of this study was to analyze the experimental uncertainty in the results of the heat transfer coefficient obtained during the vapor flow tests in micro-channels in saturation condition. Such tests were performed with mass velocity ranging from* $154 < G < 342.6\ kg/m^2s$*, removed heat flux between* $19.4 < q'' < 29.4\ kW/m^2$ *and saturation pressure from 6.8 to 9.6 bar. The extended uncertainty presented for the values of heat transfer coefficient was dh = ± 8 %.*

Keywords: *uncertainty analysis, vapor flow, micro-channels, heat transfer coefficient*

1. INTRODUCTION

The development of small and compact heat exchangers has stimulated for ~~some~~ years the studies on the boiling and condensation refrigerant in channels with small diameter. Such devices allow dissipate high heat fluxes and so they can improve the thermal performance and the reliability of small refrigeration systems, which can be applied both for automotive air conditioning and micro heat pumps and for cooling electronic devices and microprocessors. For this reason, experimental studies have focused on the thermal and hydrodynamic characteristics of boiling and condensation in reduced scale and identify the main parameters that govern boiling and condensation process, as shown by the work done by Revellin and Thome (2007), Liu and Garimella (2007), Bertsch, Groll and Garimella (2009), Tibiriçá and Ribatski (2010) and more recently by Ducoulombier *et al.* (2011), Goss and Passos (2013) and Sakamatapan *et al.* (2013).

Compact evaporators formed by mini and micro channels have been designed and developed based on the results of several works and presented as major operational advantages in relation to conventional heat exchangers tolerate high pressures and provide a larger contact area per unit volume with the fluid work. Furthermore, they allow achieving higher heat transfer coefficients for similar operating conditions.

However, there is a lack of information regarding the analysis of the experimental uncertainty obtained from literature. Apparently, this issue is not properly explored by researchers or it is not presented clearly in their works. In many cases, the experimental uncertainty of just a few parameters is merely cited in percentage terms, not demonstrating the methodology used to obtain such results. This paper aims to present a methodology for uncertainty analysis related to vapor flow in saturation condition using R134a in a test section of MPE tube. Moffat (1988) published a pioneering work on the analysis of uncertainties associated with phenomena involving heat transfer. In his work, Moffat describes in detail the uncertainties related to both parameters involved in the experiments the measurements. However, seldom propagated uncertainty analysis is well exploited in studies involving heat transfer in two-phase flows.

2. EXPERIMENTAL SET AND DATA REDUCTION

The performance of experiments involved equipment installed in the loop, as shown in Fig. 1. The circuit operates through the following steps: firstly steam of R134a is generated in the electric boiler (1), which is then directed to the pre-heater (2) used to maintain the vapor condition at the entrance of the test section The fluid is then directed to the Coriolis flowmeter (3), where the mass flow rate is measured before the entry of the test section (4). Along the test section saturated vapor is cooled without condensation and is directed to a condenser coil-type (5). Thus, the subcooled fluid is pumped through a drying filter (6) and the micro-pump (7). The mass flow rate is controlled by a by-pass (B) and by the power dissipated in the boiler which is monitored by a digital power controller and the adjustment of the pump is made through of a frequency inverter. To measure pressure of the fluid, the circuit has two absolute pressure transducers (A.P.) and a differential (D.P.), placed at the entrance and exit of the test section. Thermocouples are used in inlet and outlet of the pre-heater and test section (T) to measure the temperature of the steam, and thermocouples are placed on the surface of the test section for measuring the external wall temperature profile.

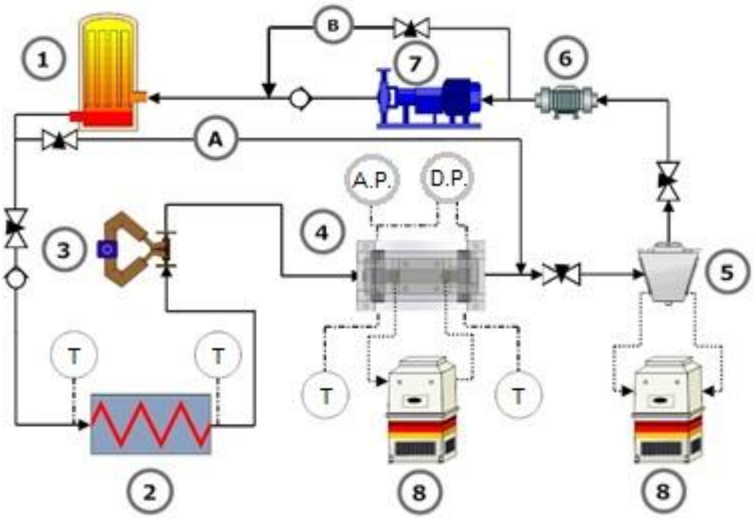

Figure 1. Diagram of the experimental setup.

The test section is shown in exploded view in Fig. 2. It is a multiport aluminum extruded tube (MPE), with eight micro-channels (a), welded ~~to~~ in two manifolds to ensure the best distribution of steam among the channels (b), ten copper plates to guarantee a thermal conductivity for the heat flux (c) and ten heat flux sensors (d). There are also two heat sinks, where water circulated from a heat bath in both its upper and lower part. The dimensional characterization of micro-channels was held in Fundação Centros de Referência em Tecnologias Inovadoras (CERTI Foundation- UFSC) through computed tomography technique; see Fig. 3, together with measurements using an optical microscope. Because it is so ductile material, the micro-channels are not all the same shape, even in the assembly they may suffer small deformations without, however, profoundly alter the areas of cross-sections of the micro-channels. The main geometrical characteristics of the test section are shown in Tab. 1.

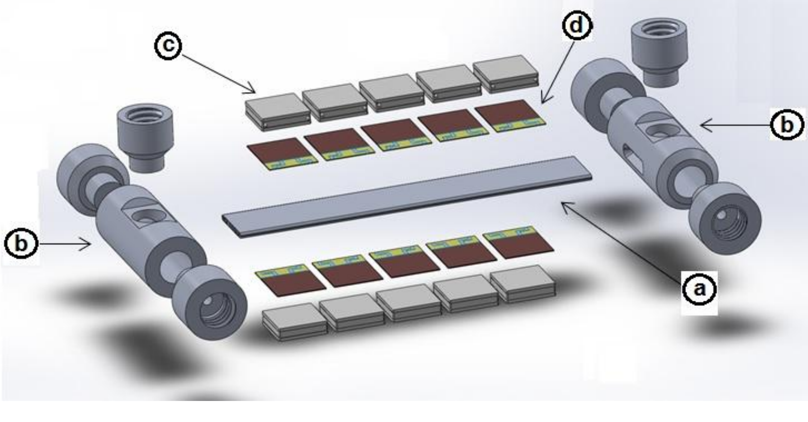

Figure 2. Exploded view of the test section containing the copper plates and the heat flow sensors.

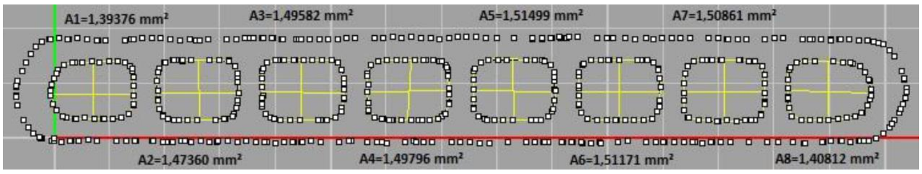

Figure 3. Areas of micro-channels measured by computed tomography.

Table 1. Characteristics of MPE.

Dimensions do MPE		
Length	98.5	mm
Width	16.5	mm
External thickness	1.5	mm
Central Channels		
Height	1.1	mm
Width	1.5	mm
Lateral Channels		
Height	1.1	mm
Width	0.45	mm
Semicircle (radius)	0.735	mm
Other Measurements		
Internal roughness	0.29	μm
Wall thickness	0.33	mm
Standard deviation	0.126	mm

2.1 Tests performed

Experimental tests were performed on the bench for heat transfer characterization in microchannels. The study with saturated vapor flow was carried out from varying the following parameters, shown in Tab. 2.

Table 2. Experimental parameters.

Parameter	Range
Mass velocity [kg/m^{2}s]	$154 < G < 342.6$
Saturation pressure [kPa]	$680 < P_{sat} < 960$
Pressure drop [kPa]	$0.462 < \Delta P_{sat} < 4.146$
Saturation temperature [°C]	$25.9 < T_{sat} < 37.8$
Heat flux removed [kW/m^2]	$19.4 < q'' < 29.4$

To ensure the absence of condensation during the tests, the inlet and exit enthalpies were calculated to establish a vapor quality in the output of the test section. In all cases, the vapor quality, obtained by interpolation of the enthalpies, was less than 3%. Thus, the presence of condensation along the walls of the test section was neglected. Such consideration is necessary due to the characteristics of the heat flow sensor.

2.2 Uncertainty of thermocouples

The measurement of temperatures throughout the experimental facility is performed via thermocouples. The uncertainty of a thermocouple E-type is in the order of ± 1 ° C, which leads to uncertainty of a very high heat transfer coefficients. Thus, the calibration of the thermocouples is necessary for decreasing this uncertainty. For this, the voltage becomes the measured quantity, instead of temperature. The efficiency of the thermocouples calibration is associated with uncertainty due to errors relating to the measurements performed by the equipment and calibration process itself. Thus, the uncertainty of the temperature obtained by the thermocouples is a combination of uncertainties involved from the following sources:

- Uncertainty data acquisition system, dT_V;
- Uncertainty of the polynomial which relates voltage and temperature, dT_d;

- Uncertainty of the bulb thermometer, dT_{termo}.

Consider the calibration curve as being a 3rd degree polynomial to determine a temperature, according to Eq. (1),

$$T(U,U_0) = \alpha(U - U_0)^3 + \beta(U - U_0)^2 + \gamma(U - U_0) + \delta \tag{1}$$

where U is the voltage of the thermocouple to be calibrated, U_0 represents the voltage measured by thermocouple immersed in a bath at zero degree Celsius (reference thermocouple). The constants α, β, γ and δ are coefficients adjusted according with the calibration of each thermocouple.

The Eqs. (2) and (3) show the derivatives of each polynomial in relation to the voltage of thermocouple to be calibrated and to the voltage of the reference thermocouple.

$$\frac{\partial T}{\partial U} = 3\alpha(U - U_0)^2 + 2\beta(U - U_0) + \gamma \tag{2}$$

$$\frac{\partial T}{\partial U_0} = -3\alpha(U - U_0)^2 - 2\beta(U - U_0) - \gamma \tag{3}$$

Since the accuracy of voltage is given by the Agilent 34970A, dU is defined by Eq. (4), in volts.

$$dU = dU_0 = \pm\left(5\times10^{-5}U + 4\times10^{-6}\right) \tag{4}$$

Then, the propagated accuracy of the polynomial equation is given by Eq. (5).

$$dT_U = \pm\sqrt{\left(\frac{\partial T}{\partial U}dU\right)^2 + \left(\frac{\partial T}{\partial U_0}dU_0\right)^2} \tag{5}$$

Another uncertainty source is associated with the reference thermometer, which measures the temperature during thermocouples calibration. This uncertainty is a combination of calibration of this thermometer (0.05 °C by the manufacturer) and its resolution, according to Eq. (6).

$$dT_{termo} = \pm\sqrt{(0.05)^2 + \left(\frac{0.05}{2\sqrt{3}}\right)^2} \tag{6}$$

Finally, there is the parcel of uncertainty that is associated to the standard deviation on the measurement made between the thermocouple and the reference thermometer, according to Eq. (7).

$$dT_d = \pm\sqrt{\frac{1}{n-1}\sum_{i=1}^{n}\left(T(U,U_0) - T_{termo}\right)^2} \tag{7}$$

Thus, the propagated uncertainty of temperature, taking into account all sources of uncertainty described above, is defined by Eq. (8).

$$dT = \sqrt{(dT_u)^2 + (dT_{termo})^2 + (dT_d)^2} \tag{8}$$

The temperatures measured in the calibration of thermocouples ranging from -10 °C to 55 °C, with an increment of 5 °C. For each temperature measured by the reference thermometer, 600 (six hundred) data points were obtained for each thermocouple. Thus, the average of propagated uncertainties of each thermocouple was in order of 0.15 °C. This value is about 85% less than the uncertainty presented by the manufacturer. The average propagated uncertainties of the thermocouples, versus temperature measured by the reference thermometer, is shown in Fig. 4. In this figure, it is clear that for several thermocouples, the propagated uncertainty was less than 0.1 °C. Anyway, we opted for the larger propagated uncertainty found during calibration for calculating the propagated uncertainty of heat transfer coefficient.

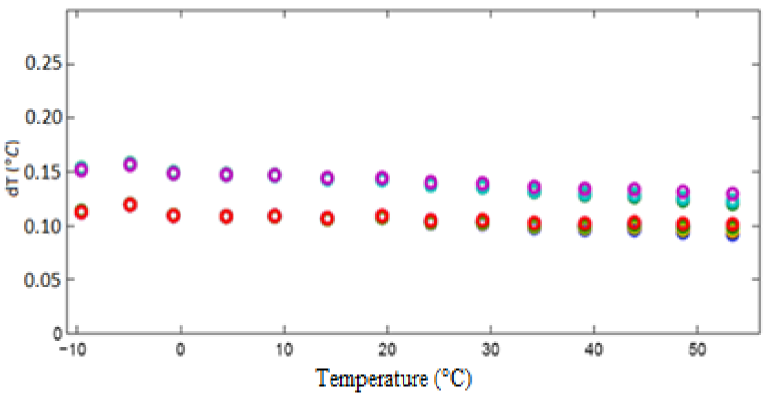

Figure 4. Accuracy of thermocouples according to temperatures during calibration.

2.3 Uncertainty of heat flux sensors

Heat flux sensors were used to measure the heat flux removed by heat sinks in contact with the copper plates, in turn, are in contact with the MPE profile. Such sensors were manufactured in Laboratório de Meios Porosos e Propriedades Termofísicas (LMPT-UFSC) having area of 15 x 15 mm^2 (the same as the copper plates) and a thickness of 300 μm. The voltage is directly proportional to the power dissipated, q, according to Eq. (9),

$$q = cU \tag{9}$$

where c represents a proportionality constant and is characteristic of each sensor, and U is the voltage measured by the sensor. Each sensor was calibrated individually, and the uncertainty, dq, is estimated at 3% of the value measured, according LMPT.

2.4 Acccuracy of heat transfer coeficient

The heat transfer coefficient is defined by Eq. (10),

$$h = \frac{q''}{\left(T_{sat}\left(P_{sat}\right) - T_{iw}\right)} \tag{10}$$

where q'' represents the heat flux measured by the heat flux sensor, T_{sat} is the saturation temperature as a function of saturation pressure. The internal wall temperature, T_{iw}, given by Eq. (11), is obtained by disregarding heat flux in the axial direction, and it is a function of the channel thickness, e, ~~of~~ heat flux sensor area, A, and of the thermal conductivity of aluminum, k_{Al}.

$$T_{iw} = T_{ew} + \frac{qe}{Ak_{Al}} \tag{11}$$

So, the propagated uncertainty of internal wall temperature is defined by Eq. (12).

$$dT_{iw} = \sqrt{\left(\frac{\partial T_{iw}}{\partial T_{ew}} dT_{ew}\right)^2 + \left(\frac{\partial T_{iw}}{\partial q} dq\right)^2 + \left(\frac{\partial T_{iw}}{\partial e} de\right)^2 + \left(\frac{\partial T_{iw}}{\partial A} dA\right)^2 + \left(\frac{\partial T_{iw}}{\partial k_{Al}} dk_{Al}\right)^2} \tag{12}$$

Due to lack of information about the uncertainty of the aluminum thermal conductivity and despising uncertainties associated to the area of heat flux sensor and the thickness of the channel, the propagated uncertainty of internal wall temperature can be described as Eq. (13).

$$dT_{iw} = \sqrt{\left(\frac{\partial T_{iw}}{\partial T_{ew}} dT_{ew}\right)^2 + \left(\frac{\partial T_{iw}}{\partial q} dq\right)^2} \tag{13}$$

Thus the uncertainty of the heat transfer coefficient is given by Eq. (14).

$$dh = \sqrt{\left(\frac{\partial h}{\partial q''}dq''\right)^2 + \left(\frac{\partial h}{\partial T_{sat}}dT_{sat}(P_{sat})\right)^2 + \left(\frac{\partial h}{\partial T_{iw}}dT_{iw}\right)^2} \tag{14}$$

3. RESULTS AND CONCLUSION

The results of the average heat transfer coefficient are shown in Fig. 5 as function of the mass velocities. A total of 195 experimental points were obtained for the heat transfer coefficient. Results obtained by Gomez (2014), in tests involving condensation, present heat transfer coefficients twice higher than those found in this work for similar mass flow rates, although the MPE profile used by the authors have more micro-channels. Sakamatapan et al. (2013) used a profile MPE similar to that used in this work and the heat transfer coefficients obtained during condensation for higher heat fluxes, are in the same range. Comparing the present results with data obtained by Goss and Passos (2013), who made a study with a circular channel with 0.77 mm Di in condensation, it is observed that heat transfer coefficients found by such authors were up to ten times higher.

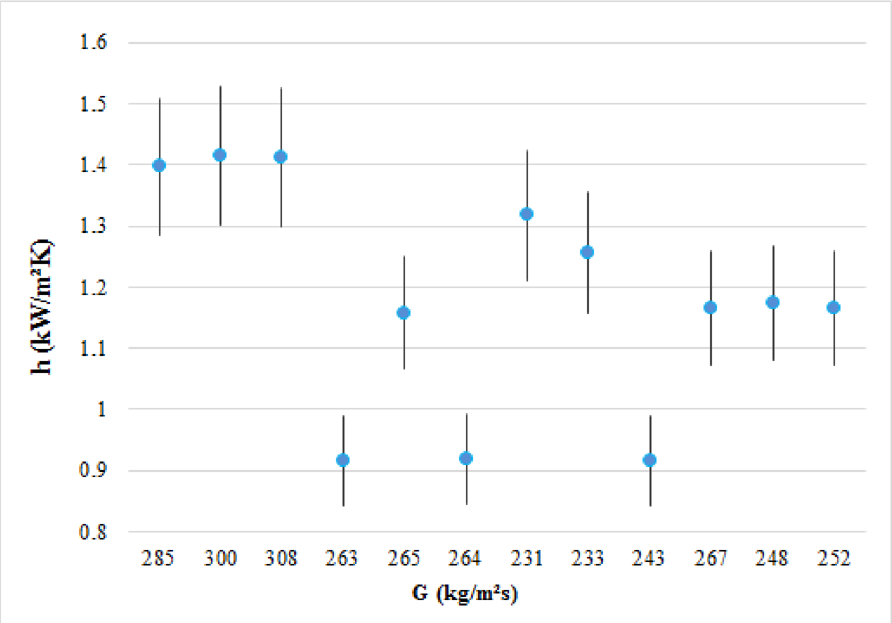

Figure 5. Average heat transfer coefficients for different mass velocities.

Through the methodology developed above, it was obtained the uncertainty of the heat transfer coefficient dh = ± 4%. Thus, the propagated uncertainty to the heat transfer coefficient can be calculated from Eq. (15).

$$u(h) = t dh \tag{15}$$

According to Eq. (15), t represents the value of the *t-Student* coefficient. To a 95% confidence interval, with infinite degrees of freedom, the uncertainty is given by:

$$u(h) = 2 \pm (4\%)$$

Finally, the propagated uncertainty obtained for the heat transfer coefficient is $u(h)$ = ± 8%. Two of the main factors that contributed to a low uncertainty are related to reduction of uncertainty in the measurement of temperature and low uncertainty of heat flux sensors.

In Fig. 6 are shown the results for the heat transfer coefficient along the channel. These results are measured in the superior and inferior walls of MPE. Such results reflect the accuracy of the measurements of heat flux and temperature on the external surface of the test section. In the study by Passos and Goss (2013), the heat flux was required by Peltier coolers and heat transfer coefficients for high vapor quality showed high uncertainty up to 70%. And only for cases with vapor quality of 40%, the uncertainty dropped to about 10%. It is important to emphasize that the methodology for the analysis of propagated uncertainties applied in this work involving single-phase flow must also be adopted for cases involving two-phase flow as boiling and condensation.

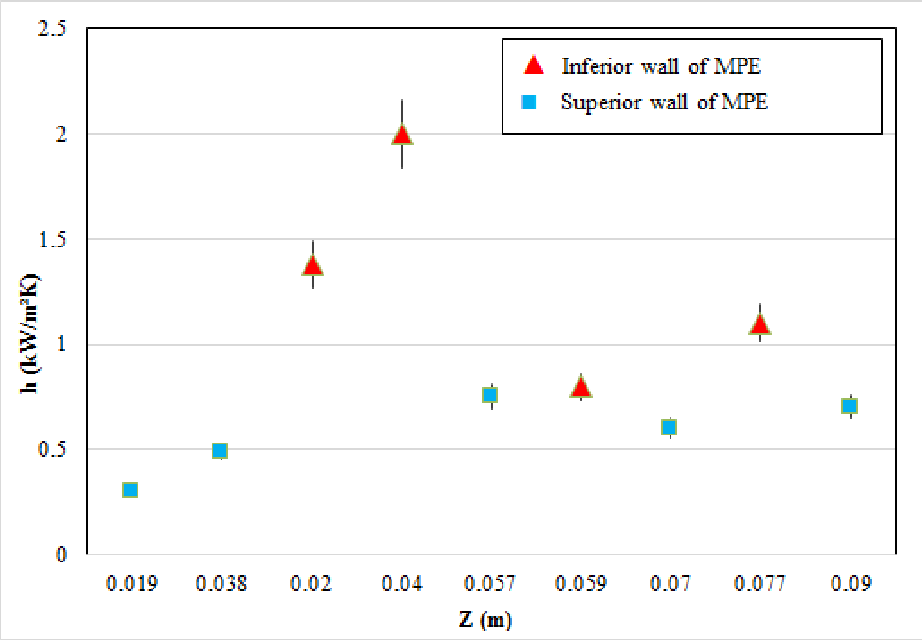

Figure 6. Variation of the heat transfer coefficient along the MPE

4. REFERENCES

Bertsch, S.S.; Groll, A.E. and Garimella, S.V., 2009. "Effects of heat flux, mass flux, vapor quality, and saturation temperature on flow boiling heat transfer in microchannels". *International Journal of Multiphase Flow*. Vol. 35, n. 2, p. 142 – 154.

Ducoulombier, M. *et al.*, 2011. "Carbon dioxide flow boiling in a single microchannel – Part II: Heat transfer". *Experimental Thermal and Fluid Science*. Vol. 35, n. 4, p. 597 – 611.

Gómez, F.I *et al.*, 2014. "Experimental two-phase heat transfer coefficient and frictional pressure drop inside mini-channels during condensation with R1234yf and R134a". *International Journal of Refrigeration*. Vol. 51, p. 12 – 23.

Goss, G.J. and PASSOS, J.C., 2013. "Heat transfer during the condensation of R134a inside eight parallel microchannels". *International Journal of Heat and Mass Transfer*, Vol. 59, p. 9 – 19.

Liu, D. and Garimella, S.V., 2007. "Flow boiling heat transfer in microchannels". *Journal of Heat Transfer*, Vol. 129, p. 1321 – 1332.

Moffat, R.J., 1988. "Describing the uncertainties in Experimental Results". *Experimental Thermal and Fluid Science*, Vol. 1, p. 3 – 17.

Revellin, R. and Thome, J.R., 2007. "Experimental investigation of R-134a and R-245fa two-phase flow in microchannels for different flow conditions". *International Journal of Heat and Fluid Flow*, Vol. 28, p. 63 – 71.

Sakamatapan, K. *et al.*, 2013. "Condensation heat transfer characteristics of R-134a flowing inside the multiport minichannels". *International Journal of Heat and Mass Transfer*, Vol. 64, p. 976–985.

Tibiriçá, C.B. and Ribatski, G., 2010. "Flow boiling heat transfer of R-134a and R-245fa in a 2.3 mm tube". *International Journal of Heat and Mass Transfer*, Vol. 53, n. 11 – 12, p. 2459 – 2468.

5. RESPONSIBILITY NOTICE

The authors are the only responsible for the printed material included in this paper.